High-Power Amplification Experiments on a Recirculating Planar Crossed-Field Amplifier

Steven C. Exelby, *Student Member, IEEE*, Geoffrey B. Greening, *Member, IEEE*, Nicholas M. Jordan, *Senior Member, IEEE*, Drew A. Packard, *Graduate Student Member, IEEE*, David Simon, *Member, IEEE*, Y. Y. Lau, *Fellow, IEEE*, Brad W. Hoff, *Senior Member, IEEE*, and Ronald M. Gilgenbach, *Life Fellow, IEEE*

***Abstract*— The recirculating planar crossed-field amplifier (RPCFA) was designed, constructed, and tested at the University of Michigan. The RPCFA was driven by a number of RF sources ranging in frequency from 2.40 to 3.05 GHz and powers of 1 to 800 kW. Pulsed voltage was delivered to the cathode by the Michigan electron long beam accelerator with ceramic insulator (MELBA-C) which was configured to supply pulses of −300 kV, 1–10 kA, with 0.3–1.0-μs pulse lengths. The RPCFA demonstrated zero-drive stability and a bandwidth of 15%. Amplification of microwave signals, at the design frequency of 3 GHz, below 150 kW, was observed with a mean gain of 7.87 dB and high variability, $\sigma = 2.74$ dB. Filtering this data set to only include shots with identical voltage and current profiles yielded a gain of 6.6 ± 1.6 dB. The mean gain increased to 8.71 dB and the variability decreased to $\sigma = 0.63$ dB when the injected microwave power increased beyond 150 kW. Peak output powers of nearly 6 MW were achieved with RF breakdown limiting the maximum output power of the device.**

***Index Terms*— Crossed-field amplifier (CFA), electron beams, high-power microwave (HPM), MAGIC, particle in cell (PIC), vacuum electronics.**

Manuscript received November 18, 2019; revised January 31, 2020; accepted March 15, 2020. Date of publication May 29, 2020; date of current version June 10, 2020. This work was supported in part by the Air Force Office of Scientific Research under Grant FA9550-15-1-0097 and in part by the L3Harris Communications Electron Devices. The work of Steven C. Exelby was supported in part by the Directed Energy Professional Society, in part by the L-3, and in part by the Air Force Office of Scientific Research (AFOSR). The review of this article was arranged by Senior Editor D. A. Shiffler.
(Corresponding author: Steven C. Exelby.)

Steven C. Exelby was with the Department of Nuclear Engineering and Radiological Science, University of Michigan, Ann Arbor, MI 48109 USA. He is now with the Air Force Research Laboratory, Albuquerque, NM 87123 USA (e-mail: scexlb@gmail.com; steven.exelby@us.af.mil).

Geoffrey B. Greening was with the Department of Nuclear Engineering and Radiological Science, University of Michigan, Ann Arbor, MI 48109 USA. He is now with Communications and Power Industries, Beverly, MA 01915-5536 USA (e-mail: geofgree@umich.edu).

Nicholas M. Jordan, Drew A. Packard, Y. Y. Lau, and Ronald M. Gilgenbach are with the Department of Nuclear Engineering and Radiological Sciences, University of Michigan, Ann Arbor, MI 48105 USA (e-mail: jordann@umich.edu; drupac@umich.edu; yylau@umich.edu; rongilg@umich.edu).

David Simon and Brad W. Hoff are with the Air Force Research Laboratory, Albuquerque, NM 87123 USA (e-mail: david.simon.23@us.af.mil; brad.hoff@us.af.mil).

Color versions of one or more of the figures in this article are available online at http://ieeexplore.ieee.org.

Digital Object Identifier 10.1109/TPS.2020.2996030

I. Introduction

THE crossed-field amplifier (CFA) is a high-power microwave (HPM) amplifier that utilizes the crossed-field configuration present in magnetrons to generate microwave gain in a compact, efficient device. Magnetrons are used in applications including radar, communications, and counter-electronics to domestic and commercial heating [1]–[3]. CFAs are commonly employed in shipboard radar and electronic countermeasure systems, where high power, efficiency, and compactness are required [4], [5].

The recirculating planar CFA (RPCFA) is the amplifying adaptation of the recirculating planar magnetron (RPM), developed at the University of Michigan [6]–[8]. The RPM features a large planar cathode surrounded by planar slow wave structures (SWSs). The SWSs are connected by semicircular recirculating bends. The increased surface of the cathode, relative to rod cathodes found in cylindrical magnetrons, allows the cathode to emit much higher currents at space charge limited densities. Additionally, this increased surface area of both electrodes allows the device to more effectively dissipate heat generated during repetitively pulsed applications. The recirculating bends effectively recycle the electron hub, maintaining high efficiency. As cavities are added to the RPM to increase the total output power generation, the volume of the magnetic fields scales linearly with the number cavities, N, opposed to N^2 as in the case of the cylindrical magnetron. This allows the device to maintain efficiency and compactness when scaled to higher power [9].

The RPCFA, diagramed in Fig. 1, is designed with the intent to retain the advantages of the recirculating planar geometry and apply them to an amplifying device. The geometry also provides advantages exclusive to CFA operation. The length of the SWS can easily be scaled to meet the needs of particular applications. The planar configuration of the device permits the RF input and output to be located physically far apart, minimizing feedback risk compared to cylindrical CFAs, where the input and output ports maybe too close together to permit high-power operation. Feedback is known to limit gain in CFAs [10]. The recirculating bends and planar drift region allow for effective demodulation of the electron hub, further reducing the propensity for feedback. Because of these

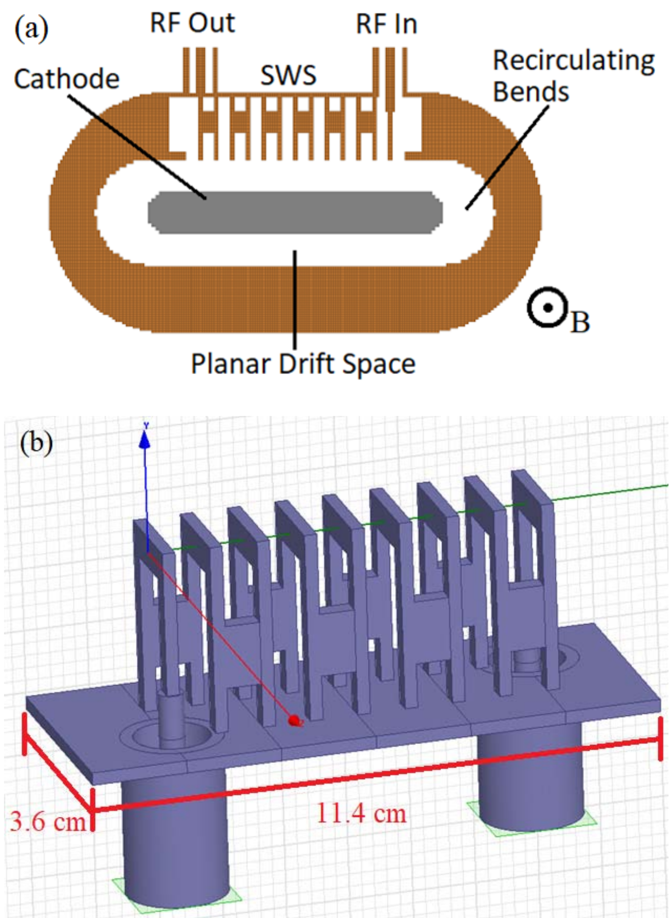

Fig. 1. (a) Labeled diagram of the RPCFA. (b) CAD rendering of SWS with coaxial input and output ports. See [22] for additional details.

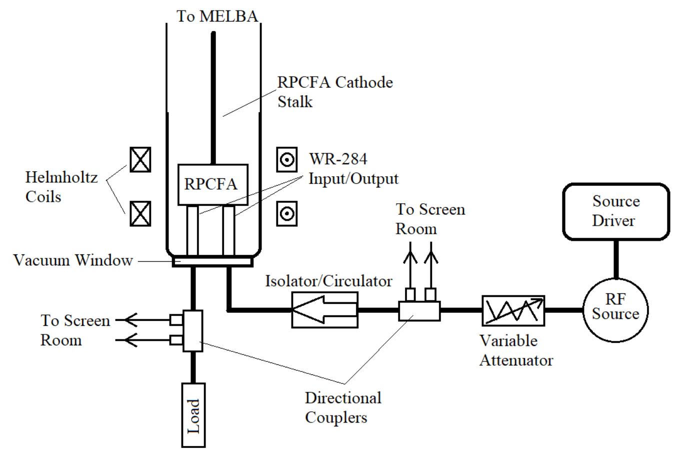

Fig. 2. Generalized experimental block diagram for RPCFA experiments. For experiments measuring amplification of a high power (∼100 kW) input RF signal, the positions of the directional coupler and the circulator were reversed to measure the reflected power.

geometric innovations, the RPCFA is expected to amplify RF signals to magnitudes typically reserved for other HPM devices [11].

II. Experimental Configuration

Amplification of an injected RF signal has been predicted in particle-in-cell (PIC) simulation [12] of a 3-GHz RPCFA using experimental parameters (such as pulsed voltage, current, and magnetic field) that can be generated in experiments conducted in the Plasma, Pulsed Power, and Microwave Laboratory at the University of Michigan [13]. A prototype RPCFA has been fabricated for experimental demonstration. A block diagram detailing a generalized configuration for all RPCFA experiments described herein is presented in Fig. 2. RF power is sampled by directional couplers. This signal is split, with half of the power sent to Hewlett-Packard (HP) 8472B low barrier Schottky diodes (0.3-dB precision) for calibrated power measurements, and the other half of the power sent to a 6-GHz, 20-GS/s Agilent 58455A oscilloscope for extracting time-resolved RF waveforms and frequency information.

Four RF sources were used to provide the input RF drive power to investigate various aspects of the device. An MG5223F magnetron (∼40 kW, 3.05 GHz) provided baseline operation at moderate input drive power at nearly the design frequency of the RPCFA (3.0 GHz). A Raytheon 4J32 magnetron (∼20 kW, 2.84 GHz) was used to test the RPCFA's response to RF drive at moderate power within the expected amplification band. An EPSCO PG5KB signal source (2.4–2.7 GHz, ∼1 kW) was used to test the amplifier's response to RF drive at reduced power and frequencies outside the expected amplification band. An MG5193 magnetron (∼800 kW, 3.0 GHz) enabled the amplification of high-power RF drive. The injected microwave power is controlled using the variable attenuator.

Pulsed voltage and current are supplied to the RPCFA by the Michigan electron long beam accelerator with ceramic stack (MELBA-C). MELBA is an Abramyan Marx bank [14], [15] currently configured to deliver pulses of −300 kV, 1–10 kA, up to 1 μs in duration [16]. Current entering the RPCFA is measured by a Rogowski coil encircling the cathode stalk and a resistive divider measures the applied voltage. Pulses typically have rise times of 100–200 ns and are crowbarred 300–400 ns after reaching full voltage. Experiments are usually conducted with a vacuum pressure on the order of 1 μTorr.

III. Experimental Results

Zero-drive stability is an important property of amplifiers, i.e., in the absence of RF input power, an output signal at appreciable power should not be generated. This was predicted in simulation [13] and was investigated experimentally by running the RPCFA without input drive. As predicted, when operated with no input signal, the RPCFA generated less than 100 W of peak RF power. The precision of this measurement is limited by the diode calibration at these low power levels. The spectrum of the raw output signal was measured directly by a 20-GS/s oscilloscope and compared to the same quantity generated in simulation, as shown in Fig. 3(a) and (b). The spectra both show broadband noise over a range of frequencies with no clear peak which would indicate free-running oscillation [17].

RF power was injected into the RPCFA using an MG5223F magnetron at approximately 3.05 GHz with 1-μs pulse lengths.

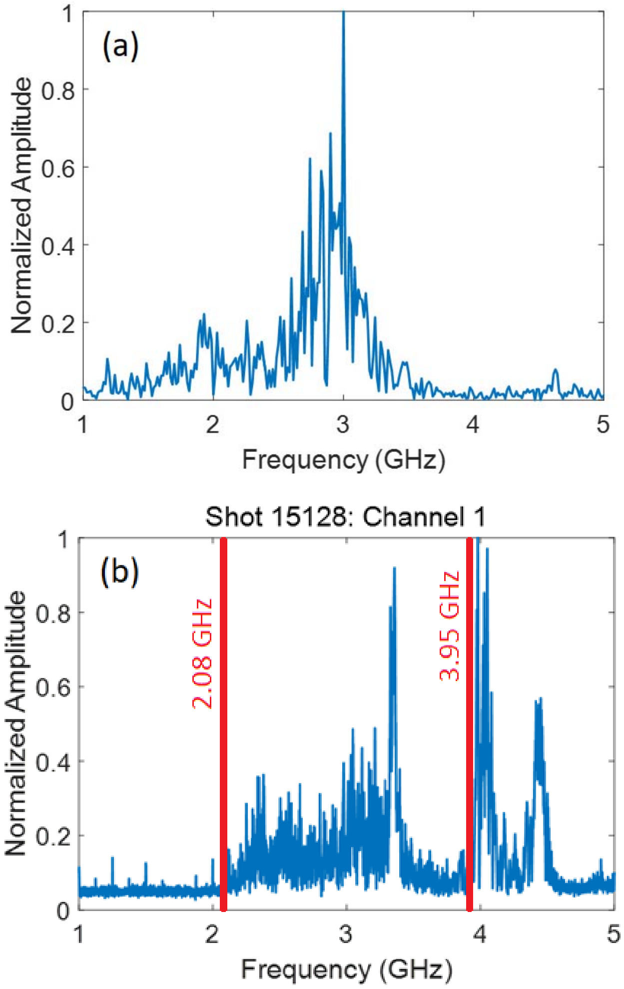

Fig. 3. (a) Spectrum of the output signal from MAGIC simulation with no injected RF drive. (b) Output frequency spectrum from the RPCFA in the absence of an injected RF drive signal. The frequency range for which the experimental measurement is calibrated is shown in red.

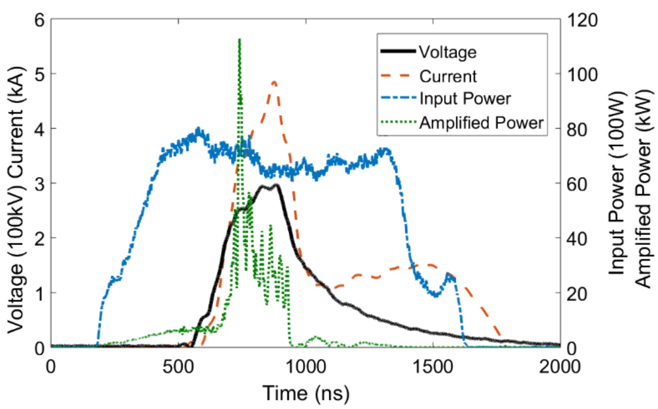

Fig. 4. Shot #15316. Amplification of a moderate (~8 kW) input RF drive.

MELBA was fired during steady-state transmission of the injected signal. The pulsed voltage and current trace synchronized with the injected and amplified RF signal are shown in Fig. 4. A moderate input power of 8 kW was amplified to 117-kW peak output, 11.7-dB gain, with the peak lasting

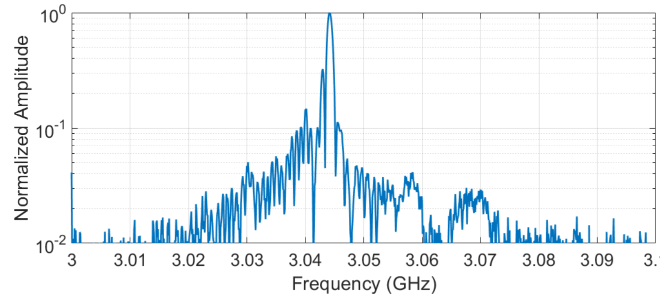

Fig. 5. Output frequency spectrum for 3.05-GHz input drive.

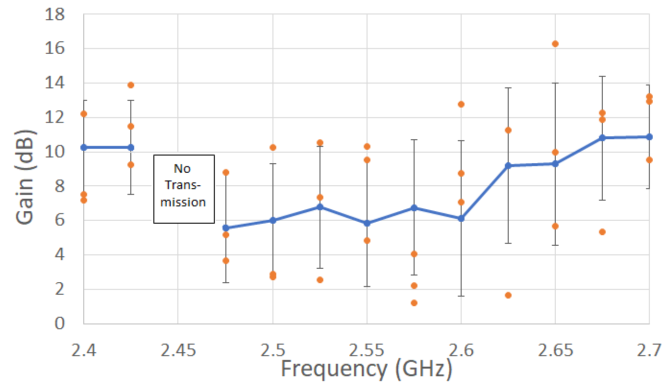

Fig. 6. Gain versus frequency using a ~1-kW RF source with continuously variable frequency. Orange dots indicate individual shots while the blue trace is a moving window average. No amplification was observed at 2.45 GHz due to severe transmission losses in the RPCFA. Decreases in gain can be associated with less severe transmission loss.

approximately 20-ns full-width at half-maximum (FWHM). After peak output is achieved the gain reduces to more modest levels (5–6 dB). Varying levels of amplification are observed for the length of the MELBA pulse and output power terminates with the fall of the pulsed voltage and current. The time-integrated spectrum of the output signal in Fig. 5 shows the dominance of the drive frequency and an absence of nondrive frequencies.

The bandwidth of the RPCFA was investigated using a source with a continuously variable frequency between 2.4 and 2.7 GHz. Measurements of gain, plotted in Fig. 6, were performed in steps of 0.025 GHz over the range and a local mean and variance were calculated. The mean gain drops 3 dB below the maximum observed mean gain at frequencies below 2.625 GHz (f_1). Although a source was not available to verify this, the RPCFA is assumed to amplify frequencies continuously over the range of 2.7–3.05 GHz (f_2), the highest frequency tested. This is predicted in PIC simulations and cold transmission measurements showing consistent transmission over the given frequency band, which are presented in [13]. Making this assumption gives a 3-dB bandwidth for the RPCFA of approximately 15% using the formula $\Delta f = (f_2 - f_1)/f_0$, where f_0 is the central frequency.

As predicted in PIC simulation, when the RPCFA was driven at frequencies below its amplification band, nondrive frequencies were not observed in the output microwave

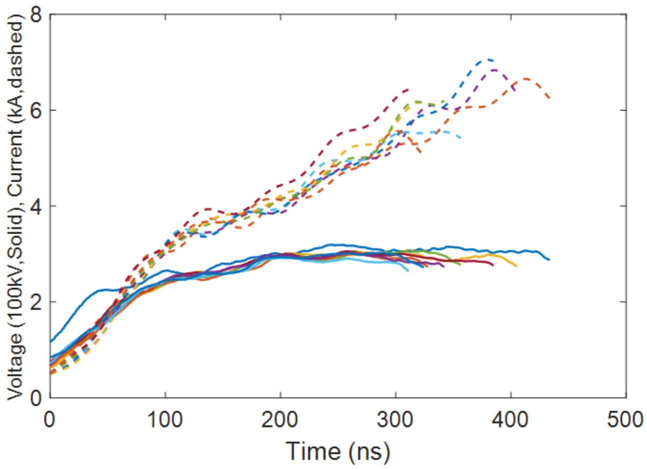

Fig. 7. MELBA voltage and current overlay for nine ideal MELBA pulses. These pulses were selected from a larger data set to determine the variation in RPCFA performance due to variation in the pulsed drive.

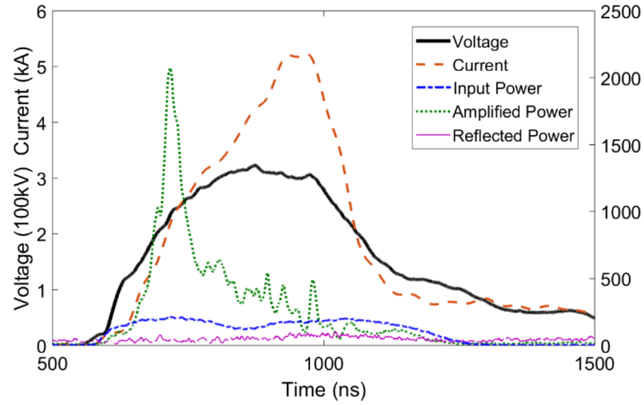

Fig. 8. Shot #16834. Amplification of a high power RF signal (200 kW) without RF breakdown.

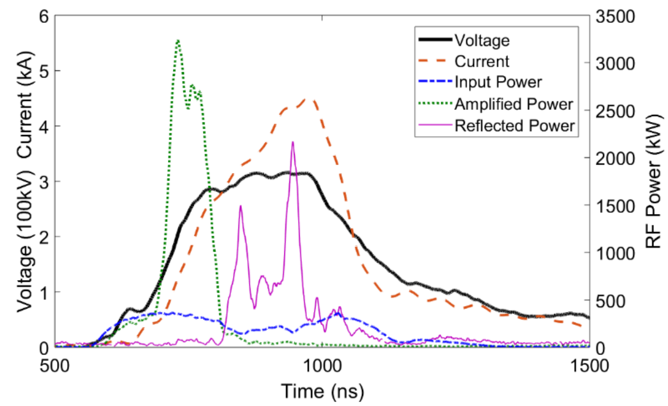

Fig. 9. Shot #16829. Amplification of a high power RF signal, around 350 kW, with RF breakdown indicated by the abrupt termination of the amplified signal and the coincident reflected signal.

spectrum. When 2.450 GHz was injected into the RPCFA, the drive frequency was not observed in the output power spectrum. At this frequency, the RF source was only capable of generating ~1 kW of RF power and the RPCFA showed significant (nearly 10 dB) transmission losses at this frequency, thought to be located at the coupling between the RPCFA and the WR-284 that transported RF power in and out of the device. The coupling was designed to work optimally from 2.7 to 3.1 GHz. The transmission losses are much less severe at 2.425 and 2.4 GHz, leading to effective amplification at these frequencies. The spectrum of the output signal closely resembled the spectrum in Fig. 3(b) indicating the RPCFA was essentially operating under zero-drive. This gives an estimate of the lower bound for amplifiable power (~100 W) in this experiment.

Undesirably high levels of shot-to-shot gain variation are evident in experiments driving the RPCFA with low input RF drive powers, as seen in Fig. 6. Variation in the shape and length of MELBA voltage pulses and the magnitude of pulsed current was significant and thought to be a contributor to the observed variation in amplification. To examine the contribution of driver variation, 80 shots were conducted with 30-kW input microwave power at 3.05 GHz and no intentional variation in experimental parameters. Overall, this data set showed a gain of 6.4 $\pm$ 2.7 dB (mean $\pm$ 1σ). Shots were filtered down to nine optimal pulses where long flat-top voltages and high current (~6-kA peak) was achieved. These pulses are synchronized according to the start time (indicated by the current reaching a designated threshold) and overlaid in Fig. 7. The data are then truncated according to the pulselength of the shortest shot to account for variation in MELBA crowbar timing. This heavily filtered data set shows a gain of 6.6 $\pm$ 1.6 dB. Thus, variation in pulsed power accounts for some of the observed variation in gain.

Up to 800 kW of microwave power was injected to the RPCFA using an MG5193 magnetron to investigate the response to high-power RF drive. The input RF pulse duration was typically around 500 ns due to the limitations of the magnetron driver. Fig. 8 shows the injected and amplified RF signals synchronized with the pulsed voltage and current. Amplification begins early in the pulse and terminates prior to the end of the pulsed power, in contrast to the behavior observed at moderate RF input drive power (Fig. 4). Both phenomena can be explained by the increase in RF field strength. Strong fringing RF fields near the input port rapidly pull electrons from the Brillouin hub into the interaction space, and back-bombard the cathode, creating an expanding plasma that increases the strength of the pulsed electric field, allowing for synchronous interaction at lower voltages than expected. The energetic bombardment of electrons reaching the anode has been shown to generate anode plasma [18]–[20]. This process can then desynchronize the electron hub from the RF wave as it progresses as well as alter the electrical characteristics of the SWS, potentially reducing its transmission rate. The result is that peak gain is achieved for a brief period of time, which then diminishes as seen in Figs. 4 and 8.

At input RF drive powers 350 kW or greater, it was observed that the amplified signal terminated abruptly and was accompanied by significant quantities of reflected RF power. A shot featuring this behavior is shown in Fig. 9. This is indicative of RF breakdown occurring on the SWS due to the intense RF

TABLE I

SUMMARY OF RPCFA RESPONSE TO VARIOUS INPUT DRIVE POWER REGIMES

RF Injected Input Power	0 – 100 W	100 W – 150 kW	150 kW – 350 kW	> 350 kW
Regime	Zero-drive	Irreproducible Amplification	Reproducible Amplification	RF Breakdown
dB Gain (mean ± 1σ)	N/A	7.9 ± 2.7	8.9 ± 0.7	8.8 ± 0.6
Description	Output power is low and no drive frequency is present in the output spectrum.	Output power is highly inconsistent but output frequency is equal to the drive frequency and the spectrum is pure	Output power is predictable and proportional to the input RF power. Spectrum is pure.	Output power is proportional to the input until RF breakdown limits the peak output power.

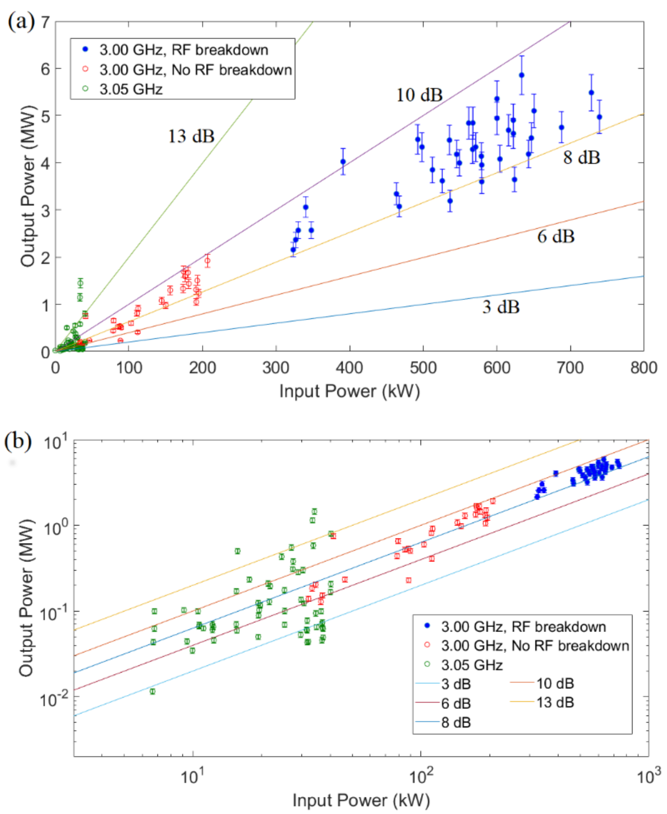

Fig. 10. (a) Peak output power versus simultaneous input power over the range of input microwave powers tested at the design frequency (~3 GHz). Gain is roughly constant over this range. (b) Peak output power versus simultaneous input power plotted on a log scale to highlight the transition from irreproducible gain at low input RF drive power to more consistent operation at higher power.

electric fields present during such high-power operation. The magnitude of reflected power is significantly greater than the input drive suggesting breakdown is occurring near the output end of the SWS. The signal is amplified as it traverses the SWS and is reflected at the point of RF breakdown. The maximum amplified output power on these RPCFA experiments is limited by RF breakdown. For especially high input RF power shots, breakdown occurs during the rise of the RF signal. The peak output power is therefore determined by RF breakdown and carries the variance of the breakdown process; however, the peak gain is consistent with values achieved below the RF breakdown threshold.

A plot of amplified RF output power versus RF input power, for 134 total shots, is presented in Fig. 10(a). Fig. 10(a) shows gain that is roughly constant over all shots at input drive powers above 150 kW. The fact that gain does not decrease at the highest drive levels indicates that the RPCFA is not near saturation at the tested power levels. A transition is observed around 150 kW of input RF power where the mean gain increases slightly and variation in amplifier gain is significantly reduced. This can be seen more clearly in Fig. 10(b). For the 84 shots where input RF power is less than 150 kW, the mean gain is 7.87 ± 2.74 dB. For the 50 shots greater than 150 kW, the mean gain is 8.71 ± 0.63 dB. A summary of the RPCFA response to four distinct input drive power regimes is given in Table I.

IV. CONCLUSION

A prototype RPCFA was fabricated to demonstrate the ability of the design to amplify HPM signals and verify the results of PIC simulation. Zero-drive stability was confirmed and a bandwidth of around 15% was demonstrated. Microwave power up to nearly 800 kW was injected into the RPCFA at the design frequency, 3 GHz. At moderate input RF power levels (<150 kW), the mean peak amplification was 7.87 ± 2.74 dB. By filtering this data set to include only optimal MELBA pulses, the gain was made slightly more consistent with a mean value of 6.6 ± 1.6 dB. At higher input microwave drive powers, the mean gain increased and the variation in gain was reduced to 8.71 ± 0.63 dB. The peak output power achievable in the experiment was around 5–6 MW and was limited by RF breakdown.

A comparison of gain versus output power for the RPCFA and some commercially available CFAs is given in Fig. 11. The RPCFA demonstrates comparable gain and output power to existing *S*-band CFAs when operated well below the RF breakdown regime (Fig. 8, shot 16834), and increased output power when allowed to operate near the mean RF breakdown limit. Rescaling the device to *L*-band would increase feature size and increase the RF breakdown limit, likely allowing for increased output power generation. The increased output power comes at the expense of efficiency. The CFAs listed in Fig. 11 are typically operated with significantly higher pulse widths and duty cycles, and may be greater than 50% efficient. The RPCFA, under typical operating conditions, reaches peak efficiencies around 0.3%, measured by taking the ratio of the

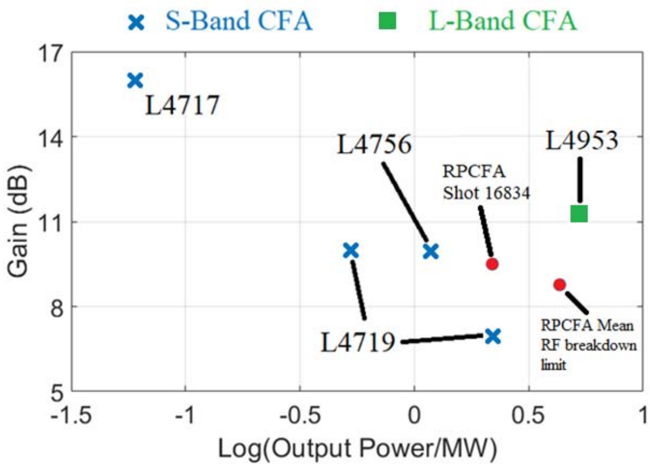

Fig. 11. Comparison to existing commercial CFAs adapted from [24].

peak power output to the instantaneous pulsed current and voltage. This reduced efficiency is primarily due to the output power of the pulsed driver compared to the RF breakdown limited peak power of the RPCFA, as well as electron endloss current [21], [22]. It is believed that peak efficiency could be increased significantly by either increasing the injected RF drive power or reducing the voltage or current of the pulsed power. In PIC simulation, endloss accounts for up to 45% of the total emitted current, a significant loss in efficiency.

While significantly higher peak powers have been reported in CFAs, such as in [23], the RPCFA experiments presented here demonstrate the viability of this novel design and offer an avenue for further development in the field of high-power amplifiers. The peak power achieved on this prototype is limited primarily by the injected RF drive. As seen in Fig. 10, the gain does not diminish at the highest injected power levels tested as is typical for CFAs near saturation. This suggests that the RPCFA is not near saturation and higher peak powers may be achievable simply by increasing the RF drive power.

References

[1] T. A. Spencer, "Current HPM source research," in *Proc. 6th Workshop High Energy Density High Power RF*, Berkeley Springs, WV, USA, 2003, p. 46.

[2] G. B. Collins, *Microwave Magnetrons*. New York, NY, USA: McGraw-Hill, 1948.

[3] R. M. Gilgenbach, Y. Y. Lau, H. McDowell, K. L. Cartwright, and T. A. Spencer, *Modern Microwave and Millimeter-Wave Power Electronics* (Crossed-Field Devices), R. J. Barker, N. C. Luhmann, J. H. Booske, and G. S. Nusinovich, Eds. Piscataway, NJ, USA: IEEE Press, 2004.

[4] W. Brown, "Description and operating characteristics of the platinotron—A new microwave tube device," *Proc. IRE*, vol. 45, no. 9, pp. 1209–1222, 1957.

[5] W. C. Brown, "Design and development of the Platinotron, Amplitron and Stabilotron," Dept. Army, Washington, DC, USA, Final Rep., Signal Corps Project No. 322A, Aug./Dec. 1955.

[6] R. M. Gilgenbach, Y.-Y. Lau, D. M. French, B. W. Hoff, J. Luginsland, and M. A. Franzi, "Crossed field device," U.S. Patent 8 841 867 B2, Sep. 23, 2014.

[7] M. A. Franzi, "Relativistic recirculating planar magnetrons," Ph.D. dissertation, Dept. Nucl. Eng. Radiol. Sci., Univ. Michigan, Ann Arbor, MI, USA, 2014.

[8] R. M. Gilgenbach, Y.-Y. Lau, D. M. French, B. W. Hoff, M. Franzi, and J. Luginsland, "Recirculating planar magnetrons for high-power high-frequency radiation generation," *IEEE Trans. Plasma Sci.*, vol. 39, no. 4, pp. 980–987, Apr. 2011.

[9] M. A. Franzi *et al.*, "Recirculating-planar-magnetron simulations and experiment," *IEEE Trans. Plasma Sci.*, vol. 41, no. 4, pp. 639–645, Apr. 2013.

[10] A. S. Gilmour, *Klystrons, Traveling Wave Tubes, Magnetrons, Crossed-Field Amplifiers, and Gyrotrons*. Norwood, MA, USA: Artech House, 2011, pp. 543–581.

[11] J. A. Benford, J. A. Swegle, and E. Schamiloglu, *High Power Microwaves*. Boca Raton, FL, USA: CRC Press, 2007.

[12] *MAGIC Electromagnetic-PIC Software*, Alliant Techsyst., Newington, VA, USA, 2014.

[13] S. C. Exelby *et al.*, "High-power recirculating planar crossed-field amplifier design and development," *IEEE Trans. Electron Devices*, vol. 65, no. 6, pp. 2361–2365, Jun. 2018.

[14] E. A. Abramyan, E. N. Efimov, and G. D. Kuleshov, "Energy recovery and power stabilization of pulsed electron beams in Marx generator circuits," in *Proc. 2nd Int. Topical Conf. High Power Electron Ion Beam Res. Technol.*, vol. 2, Oct. 1977, pp. 755–760.

[15] R. M. Gilgenbach *et al.*, "Microsecond electron beam diode closure experiments," in *Proc. IEEE Pulsed Power Conf.*, Jun. 1985, pp. 126–132.

[16] M. R. Lopez *et al.*, "Relativistic magnetron driven by a microsecond E-beam accelerator with a ceramic insulator," *IEEE Trans. Plasma Sci.*, vol. 32, no. 3, pp. 1171–1180, Jun. 2004.

[17] A. H. McCurdy, "Modification of electron cyclotron maser operation by application of an external signal," Ph.D. dissertation, Dept. Eng. Appl. Sci., Yale Univ., New Haven, CT, USA, 1987.

[18] T. A. Treado, R. S. Smith, C. S. Shaughnessy, and G. E. Thomas, "Temporal study of long-pulse relativistic magnetron operation," *IEEE Trans. Plasma Sci.*, vol. 18, no. 3, pp. 594–602, Jun. 1990, doi: 10.1109/27.55932.

[19] D. A. Shiffler *et al.*, "Effects of anode materials on the performance of explosive field emission diodes," *IEEE Trans. Plasma Sci.*, vol. 30, no. 3, pp. 1232–1237, Jun. 2002, doi: 10.1109/TPS.2002.802146.

[20] N. M. Jordan, G. B. Greening, S. C. Exelby, D. A. Packard, Y. Y. Lau, and R. M. Gilgenbach, "Pulse shortening in recirculating planar magnetrons," *IEEE Trans. Electron Devices*, vol. 65, no. 6, pp. 2354–2360, Jun. 2018.

[21] C. Leach, S. Prasad, M. I. Fuks, and E. Schamiloglu, "Suppression of leakage current in a relativistic magnetron using a novel design cathode endcap," *IEEE Trans. Plasma Sci.*, vol. 40, no. 8, pp. 2089–2093, Aug. 2012.

[22] S. C. Exelby, "Recirculating planar crossed field-amplifiers," Ph.D. dissertation, Dept. Nucl. Eng. Radiol. Sci., Univ. Michigan, Ann Arbor, MI, USA, 2019.

[23] J. Skowron, "Workshop on high-power, space-based microwave systems," Raytheon Co., Los Alamos, NM, USA, Tech. Rep., Mar. 1985.

[24] L3Harris Technologies. (2019). *Crossed-Field Amplifiers*. Accessed: Jan. 2020. [Online]. Available: https://www2.l3t.com/edd/products/cfas.htm